



## ORIGINAL ARTICLE

# Cryptotanshinone against vascular dementia through inhibition of A $\beta$ aggregation and inflammatory responses in cerebrovascular endothelial cells



Hongmei Ding<sup>a,b,1</sup>, Shu Kan<sup>b,1</sup>, Xiaolong Wang<sup>a,b</sup>, Bo Du<sup>a,b</sup>, Yingfeng Mou<sup>b</sup>, Ruiguo Dong<sup>b</sup>, Deqin Geng<sup>a,b,\*</sup>, Qichen Pang<sup>c</sup>

<sup>a</sup> Nanjing Medical University, Nanjing 210000, China

<sup>b</sup> Department of Neurology, The Affiliated Hospital of Xuzhou Medical University, Xuezhou 221000, China

<sup>c</sup> Department of Cerebrovascular, the First Affiliated Hospital of China Medical University, Shenyang 110001, China

Received 17 October 2021; accepted 3 October 2022

Available online 9 October 2022

## KEYWORDS

Cryptotanshinone;  
A $\beta_{1-42}$ ;  
Vascular dementia

**Abstract** Abnormal aggregation of amyloid- $\beta$  (A $\beta$ ) peptides and associated inflammation and apoptosis in cerebrovascular endothelial cells are prelude to inhibition of onset of vascular dementia (VaD). Although small molecules have been widely used to mitigate the cell damage induced by aggregated species of A $\beta$ , its molecular mechanism based on anti-amyloid properties and corresponding mitigation of cytotoxicity against cerebrovascular endothelial cells have not been elucidated. Herein, we used cryptotanshinone as the major bioactive compound from the root of *Salvia miltiorrhiza* Bunge to effectively inhibit A $\beta$  fibrillation and associated cytotoxicity. Thoflavin T (ThT) and 1-Anilino-8-naphthalene sulfonate (ANS) fluorescence, Congo red, and circular dichroism (CD) analyses indicated that cryptotanshinone potentially inhibit A $\beta_{1-42}$  aggregation through elongation of nucleation phase, apparent decrease in the slope of the growth phase, and the final fluorescence intensity in a concentration-dependent manner. Also, cell viability, inflammation and caspase-3 assays showed that co-incubation of A $\beta_{1-42}$  peptide with cryptotanshinone in the aggregation buffer not only mitigated their cytotoxicity, but also reduced the levels of TNF- $\alpha$ , IL-1 $\beta$ , IL-6 and caspase-3 activity in cerebrovascular endothelial cells induced by A $\beta_{1-42}$ . This study

\* Corresponding author at: The Affiliated Hospital of Xuzhou Medical University, No. 99 Huaihai West Road, Quanshan District, Xuzhou 221000, Jiangsu Province, China.

E-mail address: [gengdeqin@126.com](mailto:gengdeqin@126.com) (D. Geng).

<sup>1</sup> Contributed equally to this study.

Peer review under responsibility of King Saud University.



suggested that cryptotanshinone may show a great promise in the development of small molecule-based platforms for the treatment of VaD.

© 2022 The Author(s). Published by Elsevier B.V. on behalf of King Saud University. This is an open access article under the CC BY-NC-ND license (<http://creativecommons.org/licenses/by-nc-nd/4.0/>).

## 1. Introduction

Vascular dementia (VaD) as the second most common type of dementia after Alzheimer's disease (AD) typically originates from cerebrovascular disease (Román, 2003), during which, cerebrovascular endothelial cells are damaged (Wang et al., 2018). Cerebrovascular endothelial cell dysfunction arises before the emergence of VaD and can finally disrupt the cerebral blood flow and induce blood-brain barrier injury, followed by the upregulation of inflammatory mediators in the brain, inducing cognitive impairment (Román, 2003; Wang et al., 2018). The effects of VaD can range in severity from mild to severe. Symptoms can have a profound effect on a person's quality of life and on their ability to live independently (Román, 2003).

The evaluation of pathological markers of AD in areas of traumatic damage have suggested that amyloidogenic peptides are presented in damaged sites of the brain (Siman et al., 1989; Otsuka et al., 1991; Nakamura et al., 1992). Also, there has been a preliminary affirmation to indicate that A $\beta_{1-42}$  peptides aggregates in patients with multi-infarct dementia, and this aggregation is indistinguishable to that observed in patients with AD (Kalaria et al., 1999). These reported outcomes have crucial applications for compounds that act as potential inhibitors against amyloid formation. Indeed, aggregated forms of A $\beta_{1-42}$  peptides can be irreversibly cytotoxic against neurons and cerebrovascular endothelial cells, and inhibition of protein aggregation has been shown to prevent cerebrovascular cells dysfunction (Chi et al., 2000; Xi et al., 2012). For example, it has been shown that small molecules like potassium channel openers (Chi et al., 2000), flavonoids (Xi et al., 2012), and lutein (Liu et al., 2017) prevent A $\beta$  from production of aggregated species and relevant cytotoxicity against cerebrovascular endothelial cells. Above all, these outcomes verify the idea that aggregated species are as the crucial events causing increases in the appearance of VaD.

Traditional Chinese herbal medicine has been extensively used for the treatment of VaD (Chan et al., 2018). Cryptotanshinone is known as the major bioactive compound extracted from the root of *Salvia miltiorrhiza* Bunge, which recently used in the treatment of wide range of diseases such as cancer (Chen et al., 2013), diabetes (Kim et al., 2007), obesity (Kim et al., 2007), and neurodegenerative (Yu et al., 2007) disorders. Although, the protective effects of cryptotanshinone on some neurodegenerative diseases such as stroke and AD has been reported (Yu et al., 2007), its molecular mechanism based on anti-amyloid properties and corresponding mitigation of cytotoxicity against cerebrovascular endothelial cells as a prelude to VaD are not well understood. Herein, we explored cryptotanshinone as a promising inhibitor of A $\beta$  aggregation, leading to mitigation of cell mortality, oxidative stress and apoptosis in cerebrovascular endothelial cells.

## 2. Materials and methods

### 2.1. Materials

A $\beta_{1-42}$  was obtained from Wuhan Moon Bioscience Ltd. (Wuhan, China). Thioflavin T (ThT), 1-Anilino-8-naphthalene sulfonate (ANS), 1,1,1,3,3,3-hexafluoroisopropanol (HFIP), Fetal bovine serum (FBS) and DMEM high-glucose medium and cryptotanshinone were obtained from Sigma Chemical Co. (St. Louis, MO, USA).

### 2.2. Methods

#### 2.2.1. Amyloid preparation

The protein purification and amyloid preparation was done based on the literature (Qi et al., 2020). Briefly, A $\beta_{1-42}$  (1 mg/ml) was solubilized in HFIP followed by ultrasonication (30 min), incubation at room temperature (24 h), HFIP evaporation under vacuum, dissolution in sodium hydroxide solution, and centrifugation (15,000 rpm for 20 min) to have monomeric A $\beta_{1-42}$ . The A $\beta_{1-42}$  concentration was then measured employing UV spectrophotometry by tyrosine as a standard. Also, circular dichroism spectroscopy (CD) study was performed to examine the secondary structure of the purified protein. To explore the inhibitory effect of cryptotanshinone against amyloid formation of A $\beta_{1-42}$  (40  $\mu$ M), the protein in the tris (hydroxymethyl) aminomethane buffer (pH 7.4) was co-incubated with different concentrations of cryptotanshinone (4, 20, 40  $\mu$ M) or A $\beta_{1-42}$  alone at 37 °C for 48 h. These concentrations of cryptotanshinone were used as the lowest concentrations which may show inhibitory effects against protein aggregation.

#### 2.2.2. ThT fluorescence analysis

ThT fluorescence assay was done with a spectrophotometer (Bruker, Germany). ThT solution (25 mM) in water was prepared and filtered through a 0.22  $\mu$ m Millipore filter. A $\beta_{1-42}$  (40  $\mu$ M) samples co-incubated with different concentrations of cryptotanshinone (4, 20, 40  $\mu$ M) or A $\beta_{1-42}$  alone, were collected at different time intervals. Each sample (100  $\mu$ L) was then mixed with 900  $\mu$ L ThT solution, incubated for 15 min, excited at 440 nm and emission was recorded at 485 nm. The slit width for both emission and excitation assays were fixed at 5 nm. All assays were run at least three times to calculate the average data. The emission of the samples without protein was measured and subtracted as background from the sample. The kinetic study was also done using the relevant equation reported in the literature (Nilsson, 2004).

#### 2.2.3. ANS fluorescence intensity

A $\beta_{1-42}$  (40  $\mu$ M) samples co-incubated with different concentrations of cryptotanshinone (4, 20, 40  $\mu$ M) or A $\beta_{1-42}$  alone, were collected 48 h. Each sample (100  $\mu$ L) was then mixed with 900  $\mu$ L ANS solution, incubated for 30 min at room temperature in the dark, and excited at 380 nm and emission was recorded between 430 and 650 nm. The other experimental set up was similar to ThT fluorescence assay.

#### 2.2.4. Congo red adsorption assay

Different A $\beta_{1-42}$  (40  $\mu$ M) samples either alone or co-incubated with different concentrations of cryptotanshinone (4, 20, 40  $\mu$ M), were collected at 48 h. Then, each sample (250  $\mu$ L) was mixed with 750  $\mu$ L Congo red solution (50  $\mu$ M), and incubated for 30 min at room temperature in the dark. Afterward,

the absorbance of the samples was read between 400 and 600 nm using a Shimadzu UV-vis spectrophotometer.

### 2.2.5. Circular dichroism (CD) measurements

A $\beta_{1-42}$  (40  $\mu$ M) samples co-incubated with different concentrations of cryptotanshinone (4, 20, 40  $\mu$ M) or A $\beta_{1-42}$  alone, were collected at 48 h, diluted to the final concentration of 2  $\mu$ M, and analyzed with a JASCO spectropolarimeter (JASCO, Japan). The ellipticity changes were read from 260 to 190 nm with a scanning speed of 100 nm/min in a 0.1 cm cuvette.

### 2.2.6. Cell culture

Mouse cerebrovascular endothelial cells (bEnd.3) (CRL-2299, ATCC, USA) were cultured in DMEM containing FBS (10 %), penicillin (100 U/mL) and streptomycin (100 U/mL) at 37 °C at 5 % CO<sub>2</sub>. The bEnd.3 cells were passaged every 2–3 days to reach 70–80 % confluence. For cellular assays, cells were exposed to A $\beta_{1-42}$  samples (4  $\mu$ M) aged in aggregation buffer for 12 h either alone or with different concentrations of cryptotanshinone for 24 h, where the highest corresponding concentration of cryptotanshinone was 4  $\mu$ M.

### 2.2.7. MTT assay

Cell viability was examined via MTT assay. In brief, the cells were cultured and subjected to different A $\beta_{1-42}$  species (aged for 12 h) as described above for 24 h. 20  $\mu$ L of MTT (5 mg/mL) was then added, incubated at 37 °C for another 4 h, replaced with 150  $\mu$ L of DMSO, and finally the OD values were determined using a microplate reader (Thermo, USA) at a wavelength of 570 nm. Cell viability was then reported as a percentage of the control group treated with an aggregation buffer.

### 2.2.8. Enzyme-Linked immunosorbent assay (ELISA) to TNF- $\alpha$ , IL-1 $\beta$ , IL-6

Quantification of TNF- $\alpha$ , IL-1 $\beta$ , IL-6 in the cell culture medium was performed by TNF- $\alpha$ , ELISA kit (Abcam 108910), IL-1 $\beta$  (Abcam 197742), IL-6 (Abcam 100713) according to the manufacturer's protocols.

### 2.2.9. Caspase-3 activity assay

The cells were homogenized and protein quantification in the supernatant was done based on the Bradford assay after centrifugation. Then, 20  $\mu$ g of protein was used for determination of caspase-3 activity (Abcam 39401) according to the manufacturer's protocols.

### 2.2.10. Statistical analysis

Statistical analysis was done through one-way analysis of variance (ANOVA) with SPSS software. All results were expressed as mean  $\pm$  SD from at least three independent experiments and statistical significance was fixed at  $p < 0.05$ .

## 3. Results

### 3.1. Influence of cryptotanshinone on the fibrillation of A $\beta_{1-42}$

A $\beta_{1-42}$  (40  $\mu$ M) was incubated aggregation buffer without or with different concentrations of cryptotanshinone (4, 20,

40  $\mu$ M) at 37 °C, and A $\beta_{1-42}$  aggregated, first, by forming nucleus, then growing into oligomers and fibrils, and finally steady-state phase.

The kinetics of A $\beta_{1-42}$  aggregation in the presence of different concentrations of cryptotanshinone (4, 20, 40  $\mu$ M) or A $\beta_{1-42}$  alone were assessed by ThT assay (Fig. 1). When 4, 20 and 40  $\mu$ M cryptotanshinone were incubated with 40  $\mu$ M A $\beta_{1-42}$  monomer during fibrillization process, the fluorescence intensity of ThT was decreased in a concentration-dependent manner and was not based on the fluorescence quenching (data not shown), revealing that cryptotanshinone prevented A $\beta_{1-42}$  aggregation. It was also seen that in the presence of cryptotanshinone, the lag phases are delayed continually as the concentration of cryptotanshinone raises (Fig. 1), meanwhile, the slope of the growth phase and the final fluorescence intensity decrease in a dose-dependent fashion. These data show that cryptotanshinone has potential to inhibit A $\beta_{1-42}$  fibrillation, and the A $\beta_{1-42}$  cryptotanshinone complexes appeared in molar ratio of 1:1 can provide strongest capability to prevent the fibrillation of A $\beta_{1-42}$  (Fig. 1).

### 3.2. Influence of cryptotanshinone on the formation of hydrophobic patches of A $\beta_{1-42}$

A $\beta_{1-42}$  peptide during aggregation forms more hydrophobic patches than A $\beta_{1-42}$  monomer, promotes faster fibrillization and induces more cytotoxic effects. The influence of cryptotanshinone on the formation of hydrophobic patches of A $\beta_{1-42}$  was assessed by reading ANS fluorescence intensity. When ANS interacts with the hydrophobic patches of amyloid oligomers or fibrils, the amount of the formed hydrophobic moieties has a linear relationship with the ANS fluorescence intensity.

The ANS fluorescence emission of A $\beta_{1-42}$  samples in the presence of different concentrations of cryptotanshinone (4, 20, 40  $\mu$ M) or A $\beta_{1-42}$  alone was then determined by ANS analysis (Fig. 2). It was observed that incubation of cryptotanshinone with 40  $\mu$ M A $\beta_{1-42}$  monomer during aggregation resulted in the reduction in the ANS fluorescence intensity with an obvious red shift in  $\lambda^{\max}$  in a concentration-dependent manner. This data showed that cryptotanshinone mitigated the formation of hydrophobic patches during A $\beta_{1-42}$  aggregation and the A $\beta_{1-42}$  cryptotanshinone complexes formed in molar ratio of 1:1 can show strongest ability to prevent the formation of hydrophobic moieties of A $\beta_{1-42}$  (Fig. 2).

### 3.3. Influence of cryptotanshinone on the structure of A $\beta_{1-42}$

The Congo red interaction upon aggregation of A $\beta_{1-42}$  and appearance of  $\beta$ -sheets structures increases, which result in a significant increase in the Congo red absorbance and corresponding red shift. Therefore, the protective effects of cryptotanshinone on the formation of  $\beta$ -sheet structures of A $\beta_{1-42}$  was investigated by reading Congo red absorption intensity. Indeed, when Congo red interacts with the  $\beta$ -sheet structures of amyloid oligomers or fibrils, the amount of the aggregated species has a linear relationship with the Congo red absorption intensity.

The Congo red absorption spectra of A $\beta_{1-42}$  samples in the presence of different concentrations of cryptotanshinone (4, 20, 40  $\mu$ M) or A $\beta_{1-42}$  alone was then determined by UV-vis spectroscopy (Fig. 3). It was revealed that incubation of cryp-

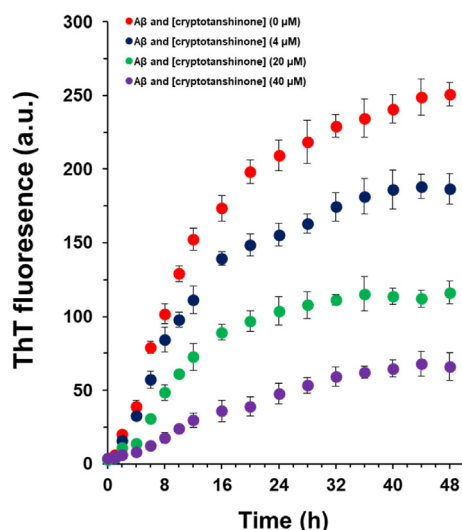


**Fig. 1** ThT fluorescence analysis of  $A\beta_{1-42}$  samples co-incubated with different concentrations of cryptotanshinone at different time intervals.

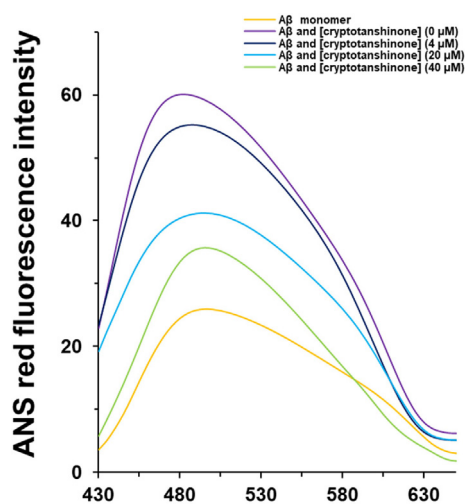


**Fig. 2** ANS fluorescence analysis of  $A\beta_{1-42}$  samples co-incubated with different concentrations of cryptotanshinone after 48 h.

totanshinone with 40  $\mu\text{M}$   $A\beta_{1-42}$  monomers during aggregation led to a remarkable reduction in Congo red absorbance with an apparent blue shift in  $\lambda^{\text{max}}$ . It was also seen this potential effect of the reduction of Congo red absorbance was done based on a concentration-dependent manner. This data displayed that cryptotanshinone mitigated the structural changes and appearance of  $\beta$ -sheets structures during  $A\beta_{1-42}$  (Fig. 3).

#### 3.4. Influence of cryptotanshinone on the secondary structure of $A\beta_{1-42}$

We then analyzed the secondary structure of  $A\beta_{1-42}$  in the presence of cryptotanshinone by circular dichroism (CD) spectroscopy study.  $A\beta_{1-42}$  displayed a disordered structure at 0 h in aggregation buffer (Fig. 4). After a 48 h incubation, the 197 nm peak as a marker of random coil conformation disap-

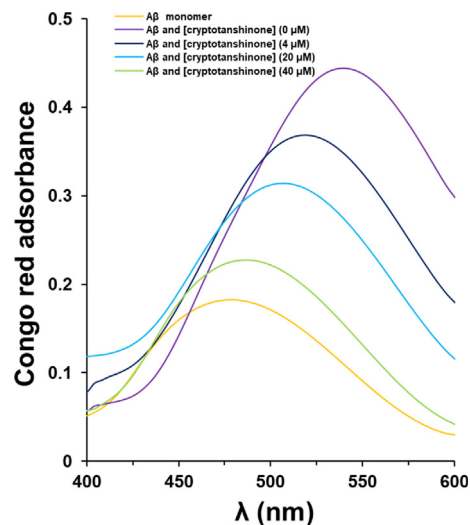


**Fig. 3** Congo red absorbance analysis of  $A\beta_{1-42}$  samples co-incubated with different concentrations of cryptotanshinone after 48 h.

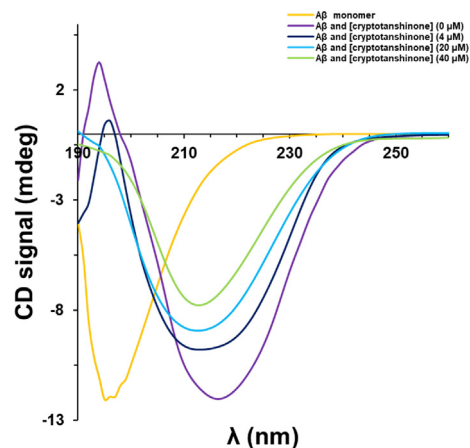


**Fig. 4** CD analysis of  $A\beta_{1-42}$  samples co-incubated with different concentrations of cryptotanshinone after 48 h.

peared and a new minimum around 216 nm was observed (Fig. 4), revealing the formation of  $A\beta_{1-42}$  aggregated species and presence of the  $\beta$ -sheet structure. After a 48 h incubation,  $A\beta_{1-42}$  in the presence cryptotanshinone showed a low number of  $\beta$ -sheet structures, and this protective effect on the secondary structural changes of  $A\beta_{1-42}$  was more effective in higher concentrations of cryptotanshinone than that of lower one (Fig. 4). This analysis indicates that cryptotanshinone were likely to inhibit  $A\beta_{1-42}$  amyloid growth in a concentration dependent manner.

#### 3.5. Effects of cryptotanshinone on cytotoxicity of $A\beta_{1-42}$ aggregated spices on bEnd-3 cells

After incubation of bEnd.3 cells with cryptotanshinone (4  $\mu\text{M}$ ),  $A\beta_{1-42}$  monomer (4  $\mu\text{M}$ ),  $A\beta_{1-42}$  aggregated (4  $\mu\text{M}$ ), or  $A\beta_{1-42}$  amyloid (4  $\mu\text{M}$ ) co-incubated with different concentrations of cryptotanshinone for 12 h, the viability of cells after

24 h was then assessed by MTT assay (Fig. 5). It was indicated that when the bEnd.3 cells incubated with cryptotanshinone, the viability of cells was not significantly reduced relative to the control group, indicating the biocompatibility of cryptotanshinone as a natural compound. However, in the presence of A $\beta$ <sub>1-42</sub> either in the form of monomeric or aggregated species, the viability of bEnd.3 cells significantly reduced relative to control cells, indicating the possibility of A $\beta$ <sub>1-42</sub> aggregation in the presence of bEnd.3 cells. On the other side, the cytotoxic effect of A $\beta$ <sub>1-42</sub> samples aged (12 h) in the presence of cryptotanshinone against bEnd.3 cells after 24 h suggested that cryptotanshinone reduced the cytotoxicity of A $\beta$ <sub>1-42</sub> samples in a concentration-dependent manner.

### 3.6. Effects of cryptotanshinone on the level of inflammatory mediators in bEnd-3 cells incubated with A $\beta$ <sub>1-42</sub>

A $\beta$ <sub>1-42</sub> samples can induce inflammatory response which promotes cellular damage and apoptosis. bEnd.3 cells were incubated with different A $\beta$ <sub>1-42</sub> species (4  $\mu$ M) either aged alone or co-incubated with various concentrations of cryptotanshinone (Fig. 6 a-c). The levels of inflammatory mediators, for example, TNF- $\alpha$  (Fig. 6a), IL-1  $\beta$  (Fig. 6b) and IL-6 (Fig. 6c) after 24 h were shown to be significantly increased after incubation of cells with A $\beta$ <sub>1-42</sub> aggregated species alone. However, it was seen that co-incubation of A $\beta$ <sub>1-42</sub> samples with cryptotanshinone aged for 12 h decreased the level of inflammatory mediators in bEnd.3 cells in a concentration dependent manner. Indeed, when A $\beta$ <sub>1-42</sub> samples aged with cryptotanshinone for 12 h, the level of inflammatory mediators decreased in the cell culture and this protective effect was more pronounced in the presence of higher concentrations of cryptotanshinone (Fig. 6 a-c).

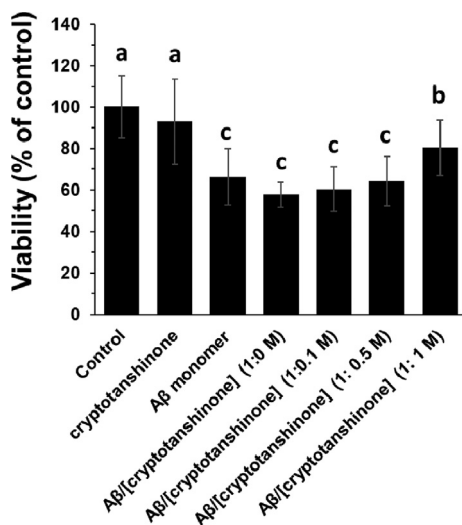


**Fig. 5** MTT assay of bEnd.3 cells upon incubation with cryptotanshinone (4  $\mu$ M), A $\beta$ <sub>1-42</sub> monomer (4  $\mu$ M), A $\beta$ <sub>1-42</sub> aggregated (4  $\mu$ M), or A $\beta$ <sub>1-42</sub> amyloid (4  $\mu$ M) co-incubated (12 h) with different concentrations of cryptotanshinone after 24 h. The letters indicated the  $p < 0.05$ .

### 3.7. Effects of cryptotanshinone on the caspase-3 activity in bEnd-3 cells incubated with A $\beta$ <sub>1-42</sub>

It was seen that A $\beta$ <sub>1-42</sub> alone aged in the aggregation buffer elevated the caspase-3 activity as an indicator of apoptosis, while the presence of cryptotanshinone in the aggregation buffer could reduce the level of caspase-3 activity induced by A $\beta$ <sub>1-42</sub> sample (Fig. 7). This data suggested that A $\beta$ <sub>1-42</sub> protects bEnd.3 cells from damage by A $\beta$ <sub>1-42</sub> (4  $\mu$ M). Therefore, the promising activity of cryptotanshinone can protect bEnd.3 cells from A $\beta$ <sub>1-42</sub>-induced inflammation and apoptosis.

## 4. Discussion

The present study showed the mechanisms underlying cerebrovascular endothelial cell dysfunction during A $\beta$ <sub>1-42</sub> aggregation as a prelude to VaD.

A $\beta$  peptides have long been considered as an effective target for treatment of neurodegenerative diseases (Maltsev et al., 2011; Tanaka et al., 2019). A $\beta$  fibrillization in the brain tissue is known to stimulate some pathological processes. Hence, inhibiting the A $\beta$  peptide aggregation with some bioactive components like small molecules could hold a great promise in the development of new therapies for neurodegenerative diseases (Tanaka et al., 2019). The exploration of cytotoxicity and the associated mechanism induced by amyloid species provides a novel impetus for the advancement of therapeutic platforms. It has been indicated that aggregated species of A $\beta$  may: i) directly stimulate synaptic dysfunction and neuronal damage, both which are as potential markers of neurodegenerative diseases initiation and progression (Reddy and Beal, 2008); and ii) induce processes like inflammation, which lead to the progression of neurodegenerative diseases (Ruan et al., 2009). Although production of A $\beta$  in the form of monomeric state is, in and of itself, a physiologically associated process, their fibrillization is pathogenic. Thus, development of potential inhibitors against A $\beta$  aggregation may lead to promising mitigation in onset of some hallmark diseases in the brain. Therefore, the approach of preventing aggregation of A $\beta$ , more specially the A $\beta$ <sub>1-42</sub> isoform, has held a great promise in disorder-modifying therapy for neurodegenerative disease (Tanaka et al., 2019).

Normally coexisting with AD, mixed VaD and neurodegenerative dementia has appeared as the main starting point of age-associated cognitive impairment. Indeed, it has been found that there is a biofunctional and pathogenic synergy between neurons, glia and cerebrovascular cells (Zlokovic, 2011; Ahmad et al., 2020), revealing a new strategy to reconsider how changes in cerebrovascular endothelial cells function could result in the neuronal damage underlying cognitive impairment (Ahmad et al., 2020). These findings call for a re-evaluation of the function of cerebrovascular factors in cognitive impairment. VaD, a brain disorder, is known as a cognitive impairment caused by cerebrovascular pathologies (Snyder et al., 2015). Furthermore, it has been disclosed that the patients suffering from different kinds of dementia have mixed pathology, consisting (amyloid plaques and ischemic lesions (Schneider et al., 2009). These findings have promoted

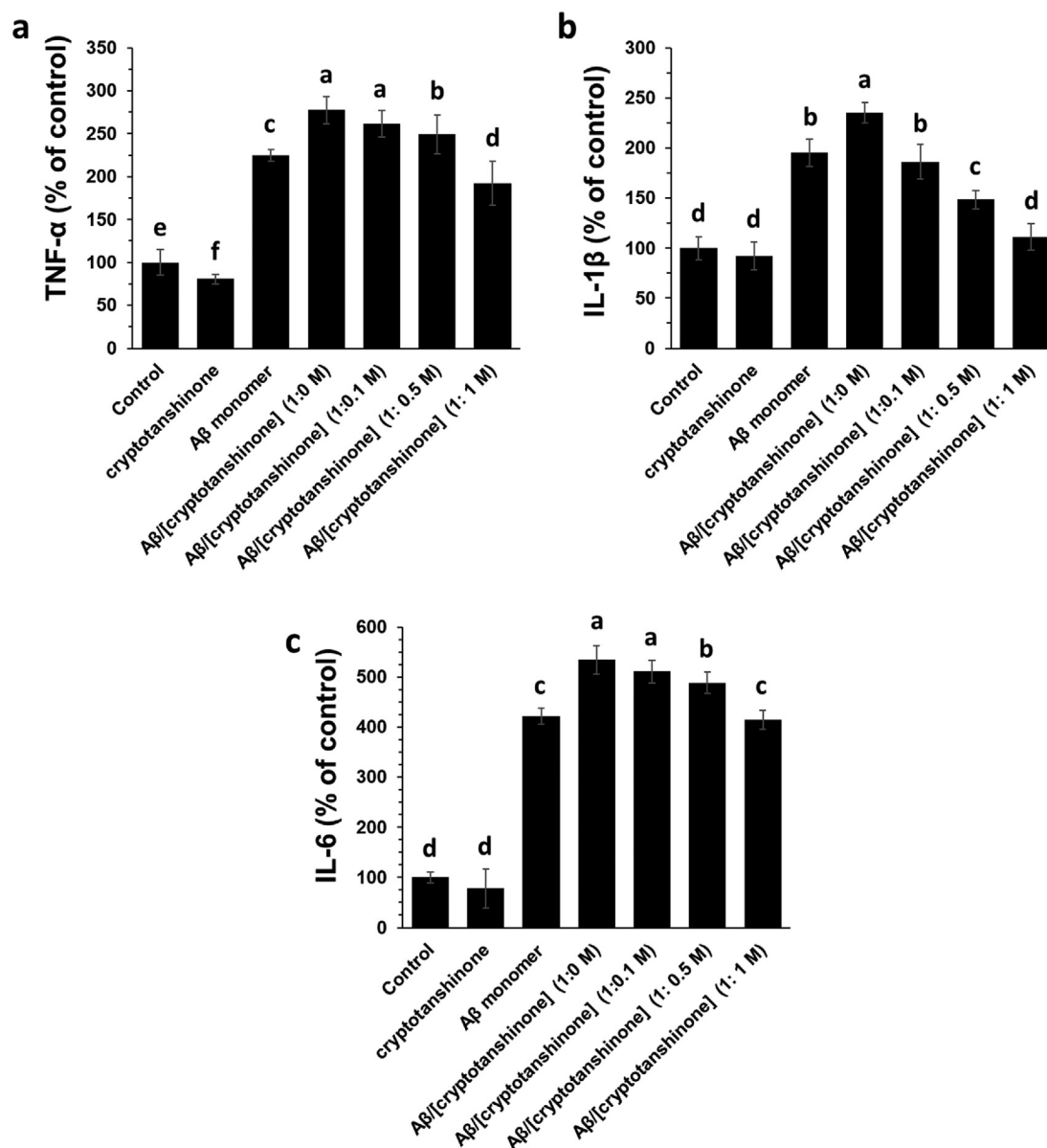


**Fig. 6** ELISA assay of bEnd.3 cells for determination of TNF- $\alpha$  (a), IL-1  $\beta$  (b) and IL-6 (c) upon incubation with cryptotanshinone (4  $\mu$ M), A $\beta$ <sub>1-42</sub> monomer (4  $\mu$ M), A $\beta$ <sub>1-42</sub> aggregated (4  $\mu$ M), or A $\beta$ <sub>1-42</sub> amyloid (4  $\mu$ M) co-incubated (12 h) with different concentrations of cryptotanshinone after 24 h. The letters indicated the  $p < 0.05$ .

a gain to potentially understand how cerebrovascular lesions influence cognition and neurodegeneration (Iadecola, 2013).

We reported that the cryptotanshinone with a polycyclic aromatic structure may interact with A $\beta$  residues and prevent its aggregation. Determining the exact residues can be considered as a key factor to be evaluated in future research efforts. It has been indicated in the literature that a compound which binds a selective subregion should meet the following potential criteria: i) it should possess moieties fitting for interacting with amino acids in, or adjacent to, the binding site; and ii) the molecule should be large enough to provide reasonable steric hindrance (Nie et al., 2011). It seems that cryptotanshinone can satisfy these criteria and therefore can be capable of inhibiting A $\beta$  fibrillization by interaction with a specific subre-

gion. In agreement with this finding, it has been reported that some typical A $\beta$  fibrillization inhibitors such as Congo red, chrysin, and curcumin provide a similar mechanism (Reinke and Gestwicki, 2007).

Also, through the comprehensive evaluation and summarization, the upregulation of inflammatory mediators and caspase-3 are suggested to serve as targets of new bioactive-based platforms for the treatment of VaD. It has been reported that bioactive compounds can mitigate cerebrovascular endothelial cell dysfunctions from A $\beta$ -triggered oxidative damage (Xi et al., 2012; Liu et al., 2017), which based on our results it may be indicated these protective effects is through apparent anti-amyloid features of small molecules like cryptotanshinone.

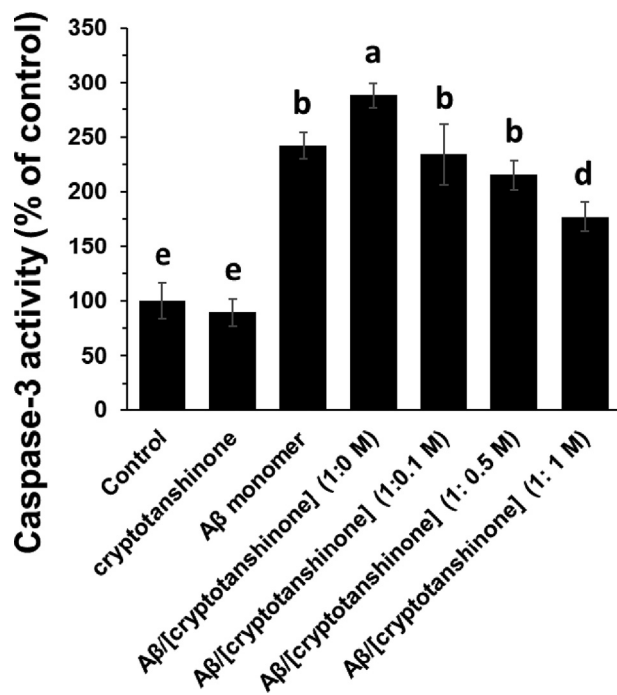


**Fig. 7** Caspase-3 assay in bEnd.3 cells upon incubation with cryptotanshinone (4  $\mu$ M), A $\beta$ <sub>1-42</sub> monomer (4  $\mu$ M), A $\beta$ <sub>1-42</sub> aggregated (4  $\mu$ M), or A $\beta$ <sub>1-42</sub> amyloid (4  $\mu$ M) co-incubated (12 h) with different concentrations of cryptotanshinone after 24 h. The letters indicated the  $p < 0.05$ .

## 5. Conclusion

In general, ThT and ANS fluorescence, Congo red, and CD analyses showed that cryptotanshinone inhibits amyloid plaque formation of A $\beta$ <sub>1-42</sub>. Additionally, cryptotanshinone showed a negligible cytotoxicity against bEnd.3 cells and also co-incubation of A $\beta$ <sub>1-42</sub> with cryptotanshinone in aggregation buffer protected the cells from inflammation and apoptosis induced by A $\beta$ <sub>1-42</sub> alone as a prelude to VaD. Future study should be done to focus on A $\beta$ <sub>1-42</sub> aggregation in vivo and the role of small molecules like cryptotanshinone in inhibition of this process. Additionally, whether cryptotanshinone can potentially cross the blood brain barrier demands further studies.

## Declaration of Competing Interest

The authors declare that they have no known competing financial interests or personal relationships that could have appeared to influence the work reported in this paper.

## References

- Ahmad, A., Patel, V., Xiao, J., Khan, M.M., 2020. The role of neurovascular system in neurodegenerative diseases. *Mol. Neurobiol.* 57 (11), 4373–4393.
- Chan, E.S., Bautista, D.T., Zhu, Y., You, Y., Long, J.T., Li, W., Chen, C., 2018. Traditional Chinese herbal medicine for vascular dementia. *Cochrane Database Syst. Rev.* 12.
- Chen, W., Lu, Y., Chen, G., Huang, S., 2013. Molecular evidence of cryptotanshinone for treatment and prevention of human cancer. *Anti-Cancer Agents Med. Chem. (Formerly Current Medicinal Chemistry-Anti-Cancer Agents)* 13 (7), 979–987.

- Chi, X., Sutton, E.T., Hellermann, G., Price, J.M., 2000. Potassium channel openers prevent  $\beta$ -amyloid toxicity in bovine vascular endothelial cells. *Neurosci. Lett.* 290 (1), 9–12.
- Iadecola, C., 2013. The pathobiology of vascular dementia. *Neuron* 80 (4), 844–866.
- Kalaria, R.N., Lewis, H.D., Thomas, N.J., Shearman, S., 1999. Brain A $\beta$ 42 and A $\beta$ 40 concentrations in multi-infarct dementia and Alzheimer's disease. *InSoc Neurosci Abstr* 23, p. 1114.
- Kim, E.J., Jung, S.N., Son, K.H., Kim, S.R., Ha, T.Y., Park, M.G., Jo, I.G., Park, J.G., Choe, W., Kim, S.S., Ha, J., 2007. Antidiabetes and antiobesity effect of cryptotanshinone via activation of AMP-activated protein kinase. *Mol. Pharmacol.* 72 (1), 62–72.
- Liu, T., Liu, W.H., Zhao, J.S., Meng, F.Z., Wang, H., 2017. Lutein protects against  $\beta$ -amyloid peptide-induced oxidative stress in cerebrovascular endothelial cells through modulation of Nrf-2 and NF- $\kappa$ b. *Cell Biol. Toxicol.* 33 (1), 57–67.
- Maltsev, A.V., Bystryak, S., Galzitskaya, O.V., 2011. The role of  $\beta$ -amyloid peptide in neurodegenerative diseases. *Age. Res. Rev.* 10 (4), 440–452.
- Nakamura, Y., Takeda, M., Niigawa, H., Hariguchi, S., Nishimura, T., 1992. Amyloid  $\beta$ -protein precursor deposition in rat hippocampus lesioned by ibotenic acid injection. *Neurosci. Lett.* 136 (1), 95–98.
- Nie, Q., Du, X.G., Geng, M.Y., 2011. Small molecule inhibitors of amyloid  $\beta$  peptide aggregation as a potential therapeutic strategy for Alzheimer's disease. *Acta Pharmacol. Sin.* 32 (5), 545–551.
- Nilsson, M.R., 2004. Techniques to study amyloid fibril formation in vitro. *Methods* 34 (1), 151–160.
- Otsuka, N., Tomonaga, M., Ikeda, K., 1991. Rapid appearance of  $\beta$ -amyloid precursor protein immunoreactivity in damaged axons and reactive glial cells in rat brain following needle stab injury. *Brain Res.* 568 (1–2), 335–338.
- Qi, Y., Yi, P., He, T., Song, X., Liu, Y., Li, Q., Zheng, J., Song, R., Liu, C., Zhang, Z., Peng, W., 2020. Quercetin-loaded selenium nanoparticles inhibit amyloid- $\beta$  aggregation and exhibit antioxidant activity. *Colloids Surf., A* 5, (602) 125058.
- Reddy, P.H., Beal, M.F., 2008. Amyloid beta, mitochondrial dysfunction and synaptic damage: implications for cognitive decline in aging and Alzheimer's disease. *Trends Mol. Med.* 14 (2), 45–53.
- Reinke, A.A., Gestwicki, J.E., 2007. Structure–activity Relationships of amyloid beta-aggregation inhibitors based on curcumin: influence of linker length and flexibility. *Chem. Biol. Drug Des.* 70 (3), 206–215.
- Román, G.C., 2003. Vascular dementia: distinguishing characteristics, treatment, and prevention. *J. Am. Geriatr. Soc.* 51 (5s2), S296–S304.
- Ruan, L., Kang, Z., Pei, G., Le, Y., 2009. Amyloid deposition and inflammation in APPsw/PS1dE9 mouse model of Alzheimer's disease. *Curr. Alzheimer Res.* 6 (6), 531–540.
- Schneider, J.A., Arvanitakis, Z., Leurgans, S.E., Bennett, D.A., 2009. The neuropathology of probable Alzheimer disease and mild cognitive impairment. *Ann. Neurol.: Official J. Am. Neurol. Assoc. Child Neurol. Soc.* 66 (2), 200–208.
- Siman, R., Card, J.P., Nelson, R.B., Davis, L.G., 1989. Expression of  $\beta$ -amyloid precursor protein in reactive astrocytes following neuronal damage. *Neuron* 3 (3), 275–285.
- Snyder, H.M., Corriveau, R.A., Craft, S., Faber, J.E., Greenberg, S. M., Knopman, D., Lamb, B.T., Montine, T.J., Nedergaard, M., Schaffer, C.B., Schneider, J.A., 2015. Vascular contributions to cognitive impairment and dementia including Alzheimer's disease. *Alzheimer's Dementia* 11 (6), 710–717.
- Tanaka, M., Saito, S., Inoue, T., Satoh-Asahara, N., Ihara, M., 2019. Novel therapeutic potentials of taxifolin for amyloid- $\beta$ -associated neurodegenerative diseases and other diseases: Recent advances and future perspectives. *Int. J. Mol. Sci.* 20 (9), 2139.
- Wang, F., Cao, Y., Ma, L., Pei, H., Rausch, W.D., Li, H., 2018. Dysfunction of cerebrovascular endothelial cells: prelude to vascular dementia. *Front. Aging Neurosci.* 16 (10), 376.

- Xi, Y.D., Yu, H.L., Ding, J., Ma, W.W., Yuan, L.H., Feng, J.F., Xiao, Y.X., Xiao, R., 2012. Flavonoids protect cerebrovascular endothelial cells through Nrf2 and PI3K from  $\beta$ -amyloid peptide-induced oxidative damage. *Curr. Neurovasc. Res.* 9 (1), 32–41.
- Yu, X.Y., Lin, S.G., Chen, X., Zhou, Z.W., Liang, J., Duan, W., Chowbay, B., Wen, J.Y., Chan, E., Cao, J., Li, C.G., 2007. Transport of cryptotanshinone, a major active triterpenoid in *Salvia miltiorrhiza* Bunge widely used in the treatment of stroke and Alzheimer's disease, across the blood-brain barrier. *Curr. Drug Metab.* 8 (4), 365–377.
- Zlokovic, B.V., 2011. Neurovascular pathways to neurodegeneration in Alzheimer's disease and other disorders. *Nat. Rev. Neurosci.* 12 (12), 723–738.